International Journal of Advanced Culture Technology Vol.3 No.1 21-30 (2015)
http://dx.doi.org/10.17703/IJACT.2015.3.1.21

IJACT 15-1-3

Polymeric Material Application for The Production of Ceramic Foam Catalyst

Anucha Sangsuriyan[1,a], Rungsima Yeetsorn[*1,2,b], Sabaithip Tungkamani[1,2,c], Thana Sornchamni[3,d]

[1] *Department of Industrial Chemistry, King Mongkut's University of Technology North Bangkok, Bangkok, Thailand*
[2] *Research and Development Center for Chemical Engineering Unit Operation and Catalyst Design (RCC), Bangkok, Thailand*
[3] *PTT Public Company Limited, Bangkok, Thailand*
[a]anucha_sy@hotmail.co.th, [b]rmy@kmutnb.ac.th, [c]sbtt@kmutnb.ac.th, [d]thana.s@pttplc.com

Abstract

Ceramic foams are prepared as positive images corresponding to a plastic foam structure which exhibits high porosities (85–90%). This structure makes the ceramic foams attractive as a catalyst in a dry reforming process, because it could reduce a high pressure drop problem. This problem causes low mass and heat transfers in the process. Furthermore, the reactants would shortly contact to catalyst surface, thus low conversion could occur. Therefore, this research addressed the preparation of dry reforming catalysts using a sol-gel catalyst preparation via a polymeric sponge method. The specific objectives of this work are to investigate the effects of polymer foam structure (such as porosity, pore sizes, and cell characteristics) on a catalyst performance and to observe the influences of catalyst preparation parameters to yield a replica of the original structure of polymeric foam. To accomplish these objectives industrial waste foams, polyurethane (PU) and polyvinyl alcohol (PVA) foams, were used as a polymeric template. Results indicated that the porosity of the polyurethane and polyvinyl alcohol foams were about 99% and 97%. Their average cell sizes were approximate 200 and 50 micrometres, respectively. The cell characteristics of polymer foams exhibited the character of a high permeability material that can be able to dip with ceramic slurry, which was synthesized with various viscosities, during a catalyst preparation step. Next, morphology of ceramic foams was explored using scanning electron microscopy (SEM), and catalyst properties, such as; temperature profile of catalyst reduction, metal dispersion, and surface area, were also characterized by H_2-TPR and H_2-TPD techniques, and BET, respectively. From the results, it was found that metal-particle dispersion was relatively high about 5.89%, whereas the surface area of ceramic foam catalysts was 64.52 m^2/g. Finally, the catalytic behaviour toward hydrogen production through the dry reforming of methane using a fixed-bed reactor was evaluated under certain operating conditions. The approaches from this research provide a direction for further improvement of marketable environmental friendly catalyst production.

***Keywords**: Polymeric sponge method, Dry reforming, Ceramic foam catalyst, Polymeric catalyst template, Hydrogen production, Sol-gel method*

Manuscript Received: Feb. 10, 2015 / Revised: Mar. 13, 2015 / Accepted: Apr. 20, 2015
Corresponding Author: anucha_sy@hotmail.co.th
Tel: +66 2470 8000, Fax: +66 2470 8412
Department of Industrial Chemistry, King Mongkut's University of Technology North Bangkok

1. INTRODUCTION

Sometime between the years 2015 and 2020, the world fossil fluid fuel demand will outstrip production, which will precipitate the requirement for increased use of sustainable alternative fuels and energies such as hydrogen fuel cells. Consequently, hydrogen becomes requisite fuel. One of hydrogen productions widely studied in literatures is from the dry reforming methane (DRM) because the dry (CO_2) reforming of methane is a well-studied reaction that is of both scientific and industrial significance. Catalysts necessitate the DRM process to achieve high hydrogen productivity and the most extensively catalysts used for DRM are based on Ni [1]. The rate of DRM reaction is affected not only by the types of active metals and catalyst supports but also by shapes of catalysts. There are several types of catalysts, for instance, pellet, spherical particle, monolith, and ceramic foam [2]. This work was addressed on a ceramic foam catalyst fabrication for DRM due to an interesting structure of the ceramic foam. A ceramic foam has sponge-like structures that characteristically have open accessible pores in the range 10 to 100 $inch^{-1}$[3], and an interconnecting porosity in the range 75– 90%[3]. Accordingly, the ceramic foam catalyst is more appropriate for DRM than the conventional pellet and spherical catalysts due to lower pressure drop, higher external mass transfer rates, and larger efficiency factors for pore-diffusional regimes [4]. In a comparison with a monolith catalyst, the ceramic foam catalyst can create greater turbulence gas flow during the reaction, whereas; the monolith catalysts create more laminar gas flow. The ceramic foam structure creates tortuous flow paths which generate considerable the turbulence flow. The turbulence flow will increase convective heat transfer and enhance opportunity and time for reactant gases to contact active sites of catalysts [4], as indicated in Fig. 1.

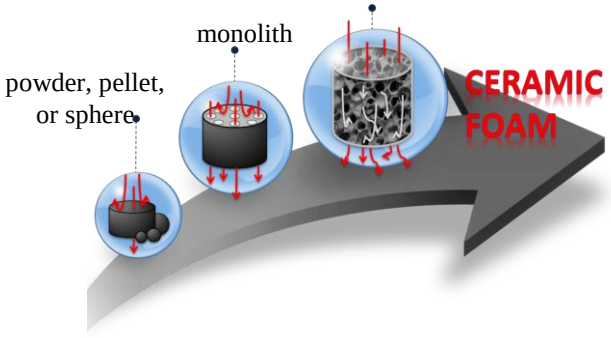

Figure 1. The pictorial model of mass transfer in various shapes of catalysts

Ceramic foams can be formed following different manufacturing approaches[5], for example, gel casting, hollow bead, and the reticulated sponge techniques. The first route, ceramic powder slurry is transformed in solid ceramic foam by introducing foaming agent into ceramic solution, however; the final structure of ceramic foam is barely controlled. The second method is a process using mold to shape ceramic foam, nevertheless; the final structure is almost like a monolith structure. The last one is the most conventional method to produce ceramic cellular structures. During this process the ceramic structure is stabilized and failure of smaller pores would be prevented, thus the final product is preferred ceramic foam. This work was interested in a manufacturing route that involves loading preformed plastic foam or a polymeric template with aqueous oxide slurry. From a hypothesis, optimum parameters could benefit to produce a replica of the original structure of polymeric foam. In terms of a catalyst preparation, a sol–gel technique was selected for ceramic foam catalyst production for this research, since the method has several advantages such as a well-defined pore size distribution, high purity control of reactants, large and controlled porosity combined with the capability to form large surface area [6]. Furthermore, catalysts produced from sol-gel technique have

resistance to deactivation, high thermal stability, high metal dispersions, and high thermal resistance. The main objective of the present study was to investigate the preparation and characterization of a sol–gel nickel–alumina catalyst which is a ceramic foam catalyst, and to evaluate their potential in the DRM reaction. The ceramic foam was generated by the reticulated sponge technique using a polymeric template. To create the ceramic foam which has the same structure as the polymeric structure, there were many effects that must be investigated, such as a polymer foam structure, viscosity of catalyst solution, and the ability of polymer foam to absorb catalyst gel, dispersion of the active metal, and the sintering rate, etc.

2. EXPERIMENTAL METHODOLOGY

2.1 Polymeric foam selection and characterization

Prior to the catalyst preparation, it is important to select proper polymeric foam. The selection relates to two main reasons; an appropriate polymeric foam structure corresponding to a required structure of a final ceramic foam catalyst and providing a direction for further improvement of marketable environmental friendly catalyst production. Therefore, four types of industrial waste foams; Polyurethane (PU), Polyvinyl alcohol (PVA), Expanded polyethylene (EPE), and Expanded polypropylene (EPP), from furniture and packaging industries were collected to observe their microstructures. Several microstructural features of the polymeric foams were determined using Optical Microscope (BH2-UMA, Olympus) and images were interpreted via analysis software (SemAfore 5.21) to determine pore size, pore density, and strut size. Morphological studies of useable polymeric foam samples were made by Scanning Electron Microscope (JSM 7600 F, JEOL). Moreover, the porosity of foams was also determined using Gas pycnometer technique following ASTM D6226. Decomposition temperatures of polymeric foam specimens were determined by the use of Thermogravimetric Analyser (TGA/DSC1, Mettler Toledo) for setting sintering rate in a catalyst preparation step.

2.2 Ceramic foam catalyst preparation

10NAM catalyst was prepared via a sol-gel method, and then the catalyst was coated on polymeric foam template to produce a ceramic foam catalyst. The template was coated by 10NAM slurry, and template pores were filled with aqueous slurry of a ceramic material. After squeezing out the excess slurry, the impregnated catalysts were aged in air at room temperature for 48 h. After this period, the catalyst was dried at 80 ^{o}C for 24 h. The polymer was calcined and the Al fraction was oxidized in air at temperatures above 1000 ^{o}C. The polymeric template decomposed during the calcination, while the ceramic particles were sintering. Finally, the ceramic form replaced the original foam (Fig. 2 exhibits the overall process).

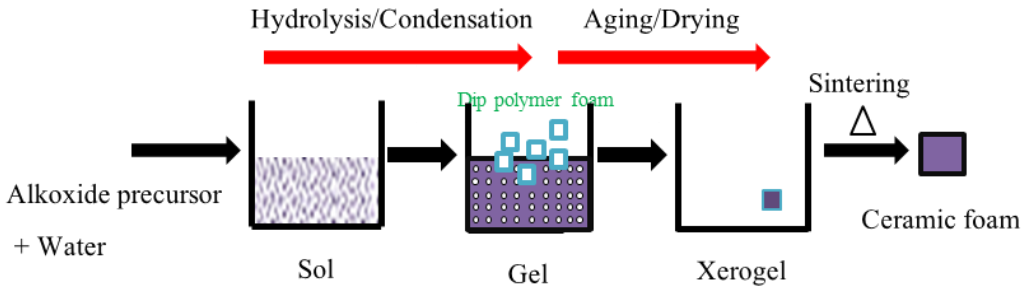

Figure 2. The overall process of ceramic foam catalyst preparation

2.3 Rheological measurements of aqueous oxide slurry

The rheological behaviour and viscosity of ceramic slurry with different water contents were investigated using a digital rotational viscometer (Brookfield, PROGRAMMABLED V-II).

2.4 Ceramic foam catalyst characterizations

The morphological micrograph of 10NAM ceramic foam was observed by SEM. Please note that specimens were coated with a very thin Au/Pd layer in order to improve the electrical conductivity of the sample surface. In terms of catalyst surface, the specific surface area of ceramic foam catalysts was determined by BET model via nitrogen adsorption at -196 ^{o}C, and approximate 0.2 g of catalyst was used for each analysis. The degassing temperature was 350 $^{\circ}$C to remove the moisture and other adsorbed gases from a catalyst surface. Moreover, the temperature-programmed reduction of H_2 (H_2-TPR) was carried out, and the procedure used 0.2 g. of fresh catalysts for testing. The catalysts, which had been thermally treated under Ar stream at 220 $^{\circ}$C for 30 min to remove water and other contaminants, were heated from 40 $^{\circ}$C to 800 $^{\circ}$C at a rate of 10 $^{\circ}$C /min in 30 ml/min of 5% of H_2/Ar and maintained at 800 $^{\circ}$C. During this test hydrogen consumption was monitored. The temperature-programmed desorption of H_2 (H_2-TPD) was also performed after the TPR experiments. The procedure was performed using a temperature-programmed multipurpose unit with a TCD detector where the catalyst samples (0.2 g) were first reduced with pure hydrogen (30 mL/min) at a heating rate of 1 $^{\circ}$C /min. After the temperature reached 700 $^{\circ}$C for 4 h., pure hydrogen flow was switched to pure Ar. The sample was cooled to room temperature, and then the gas flow was changed for pure hydrogen. Next, the H_2 flow was switched to a 25 mL/ min Ar flow. After 30 min in Ar flow at this temperature, the sample was heated to 900 (10 $^{\circ}$C /min, after reaching 40 $^{\circ}$C), and desorption of hydrogen was monitored.

2.5 Catalytic perormance tests

The dry reforming of methane was carried out for 6 h at 620 $^{\circ}$C in a fixed-bed continuous flow reactor containing 0.5 g of fresh catalyst. The reactant, which was a gaseous mixture of CH_4 and CO_2, was supplied with 60 ml/min ($CH_4/CO_2/N_2$=15/25/20) of a flow rate. Operating temperature was measured with a thermocouple placed in a catalyst bed. Prior to the reaction, catalysts were pre-treated under N_2 stream at room temperature for 30 min to remove other contaminants. They were also activated with 30 ml/min of H_2 flow under 620 $^{\circ}$C for 20 h. After the reduction, the reactor was adjusted to 700 $^{\circ}$C of reaction temperature. Throughout the reaction, out let gas was online analysed every 20 min by GC (Agilent 6820) equipped with TCD detectors using Air zero, N_2 and He as carrier gases.

3. RESULTS AND DISCUSSIONS

3.1 Polymeric foams characterizations

Foam structure typically comprises cells, which generally have two types; open and close cells, plateau borders, and struts [3] as indicated in Fig. 3. Foam structures classically depend on a process creating bubbles and foaming agent sorts. Physical structures of PU, PVA, EPE, and EPP foams were perceived by digital images (Fig.4 (a-d)) and optical micrographs (Fig.4 (e-h). The results clearly demonstrate that the studied polymeric foams have different cell structures. EPE and EPP foams appear the unconnected thin fibre/membranes blocking each cell which is called the close cell, while PU and PVA structures contain many open interconnecting cells. To make the results clearly, porosity of polymer cells were considered using gas pycnometer. The results in Fig. 5 (a) indicate that PU has highest porosity which is approximate 99% followed by PVA 98%, EPP 69% and EPE 43%, respectively. The results of the foam porosity, the image analysis, and the observation of absorb 10 NAM slurry uptake are given to serve as a guide in selecting of polymer foam templates which must be immersed in ceramic slurry. Close cells badly absorb

slurry, while the slurry can easily move into polymer foam pores containing interconnecting open cells. The correlated results are in a reasonable agreement that EPE and EPP foams are not suitable for the ceramic foam preparation. Consequently, PU and PVA were handpicked for further exploration.

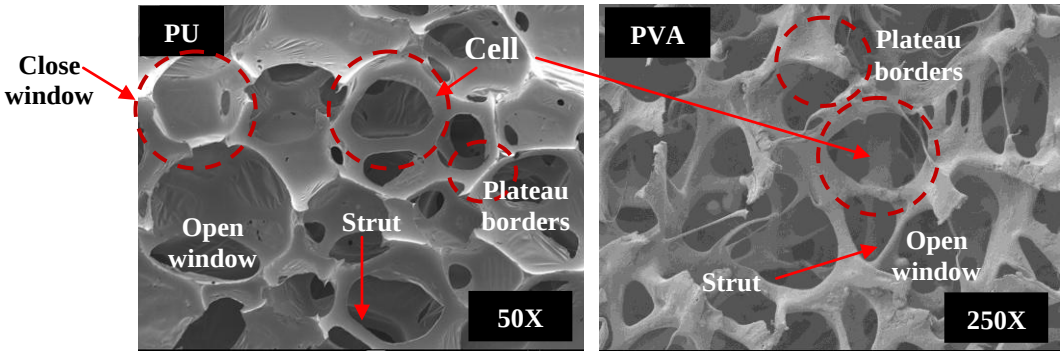

Figure 3. SEM micrographs of PU and PVA show cell structures

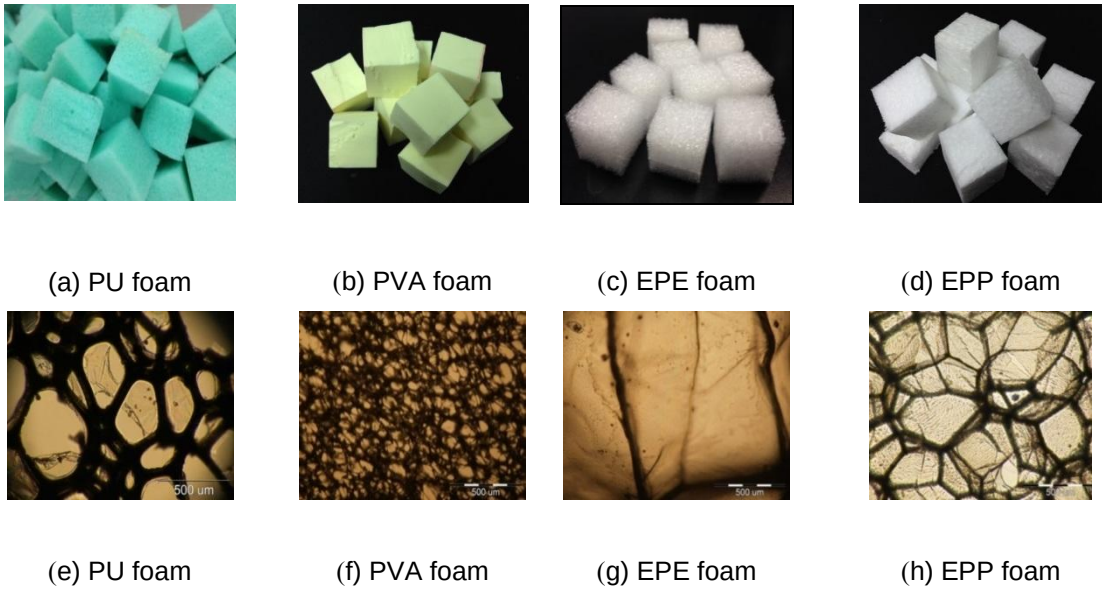

(a) PU foam (b) PVA foam (c) EPE foam (d) EPP foam

(e) PU foam (f) PVA foam (g) EPE foam (h) EPP foam

Figure 4. Digital images of polymer foams (a-d) and OM images (5X) of polymer foams (e-h)

Fig. 5 (b) and Fig. 3 illustrate that both PU and PVA have the similar porosity values, but the average cell size of PVA is smaller than the size of PU. The small cell size affects ceramic slurry adsorption and influences flow transport of ceramic slurry. It can be explained that a reduction in pore size results in smaller passage for fluid permeation [7]. In terms of a strut size, one big advantage of cells encompassing big struts could be realized with sufficient strength of ceramic foam products [8].

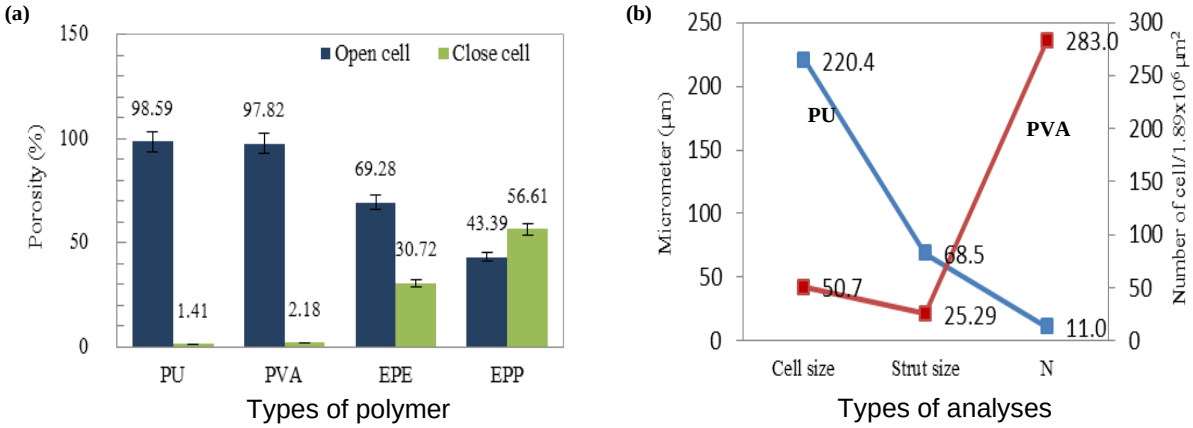

Figure 5. (a) Porosity values of polymer foam templates (b) Structure analyses of PU and PVA foam templates

3.2 Rheological measurements of aqueous oxide slurry

Beside the structure of foam, rheological behaviour would affect on 10NAM coating performance and also catalyst metal dispersion. Therefore, viscosity of ceramic slurry prepared through the sol-gel process with different water contents was investigated.

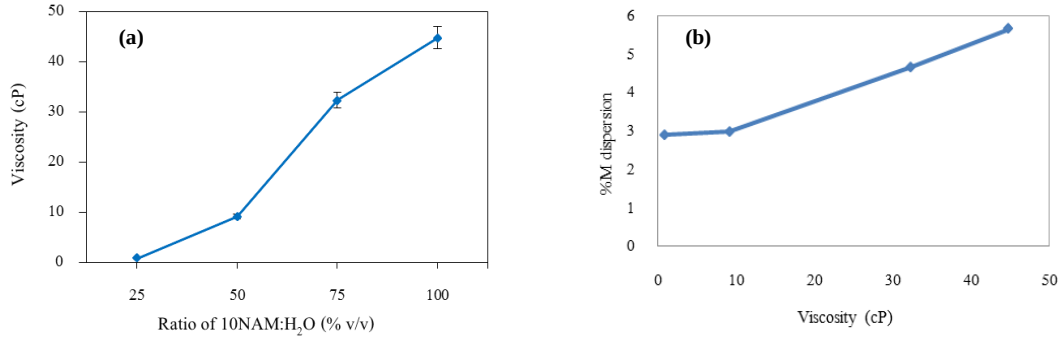

Figure 6. Relation of water contents in 10NAM slurry and its viscosity (a) and relation of viscosity and metal dispersion (b)

As seen in Fig. 6 (a), the viscosity values of 10NAM ceramic slurry has tendency in decrease with the dilution of ceramic slurry increases. Although all samples; 10NAM: H_2O = 100:0, 75:25, 50:50 and 25:75 (%v/v), could be used for sol-gel process, the relation between flow behaviour and metal dispersion should be concerned. As acknowledged, the metal dispersion directly impacts on a catalyst performance. The metal dispersion values of samples with different water contents were monitored via H_2-TPD analyses as Fig. 6 (b). The data from areas under the peaks of TPD profile illustrate that a decrease in viscosity from 44.83 cP to 0.94 cP decreases metal dispersion on catalyst support. Typically, the flow of fluid with higher viscosity will give better dispersion of solid particles, while the flow of diluted fluid will give better distribution. When water contents increased active metals could distribute to overall areas, but the metal would agglomerate each other [9]

3.3 Ceramic foam catalyst characterizations

The hydrogen TPD profiles (Fig. 7(b)) of the samples present hydrogen evolution during heating. All ceramic foam catalysts show consistent in desorption. The hydrogen consumption peak can be separated into two temperature ranges which are 120-400 ◦C and 400-900 ◦C. The results designate that 100CF-10NAM gives the highest hydrogen desorption. This result reaches agreement with the metal dispersion values and catalyst surface areas. The results from BET illustrate that 100CF-10NAM has highest surface area (51.12 m^2/g), and the surface area trends to reduce with the water contents in catalyst slurry rises.

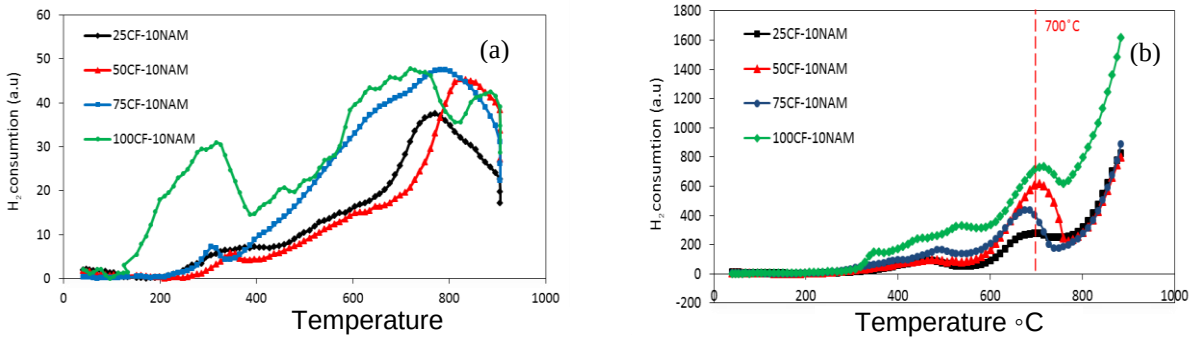

Figure 7. TPD (a) and TPR (b) profiles of ceramic foam catalysts(xCF-10NAM, x = 100:0, 75:25, 50:50 and 25:75) made from a PU foam template, and they were calcined under 1050 ◦C with 5 ◦C /min of a heating rate

Fig. 7 (b) presents the TPR profiles of oxides obtained by the sol–gel method. By analysing these curves, it is possible to obtain information regarding the types of interactions that occurs between the oxide of the active metal and the catalytic support [10]. The growth of metallic nickel particles during the reduction process depends on the interactions between NiO species and the support, as well as Ni^{2+} ions in the Mg(Al)O structure[11]. According to the TPR profiles, the peaks in the temperature range 400–600 ◦C are attributed to the reduction of Ni^{2+} in the NiO phase. Its complexity may be ascribed to the presence of dissimilar NiO species. On the other hand, TPR peaks at about 700 ◦C are associated with the reduction of Ni^{2+} in $NiAl_2O_4$ [12]. In these experiments a maximum reduction temperature of 700 ◦C were adopted for the H_2-TPD technique in order to complete reduction of all the Ni species. The thermal stability of modified PVA was evaluated from TGA under air, recorded at 5 ◦C /min. TGA curves were plotted against temperature (Fig. 8(a)). PU starts its degradation from approximate 246-636 ◦C where isocyanate is removed from polymer chains, and the decomposition of monomers and polyol molecules occurs in the next stage.

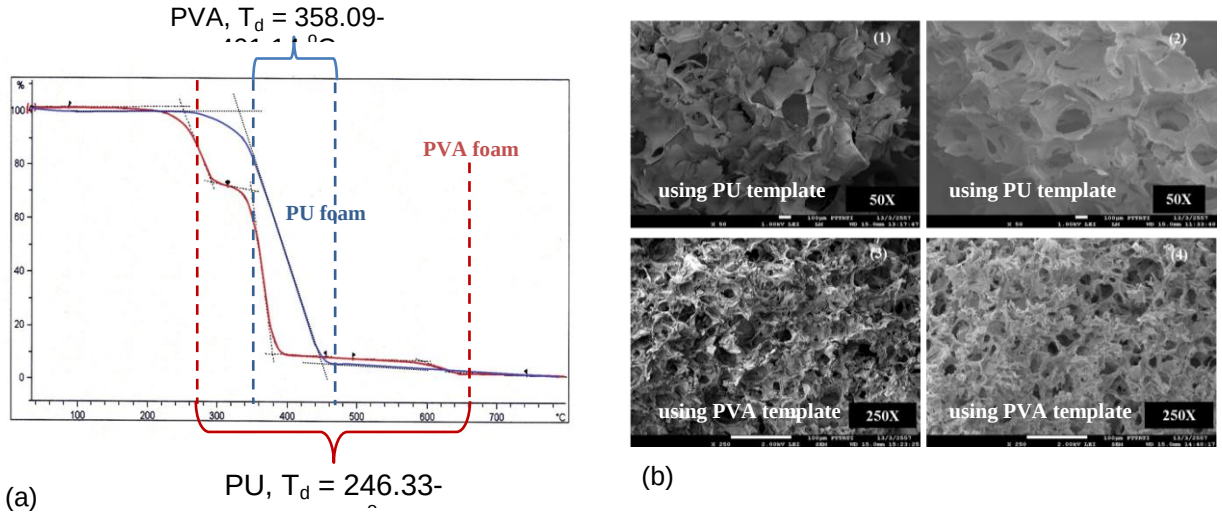

Figure 8. TGA thermogram of PU and PVA foams (a) and their SEM micrographs (b); (1) 5-0.5-5 ◦C/mim, (2) 5-5-5 ◦C/mim, (3) 5-0.5-5 ◦C/mim, (4) 5-5-5 ◦C/mim

In the case of PVA, its decomposition begins after losing water (358.09 - 491.14 ◦C) where hydroxyl groups and polymer chains are degenerated [13]. The polymer decomposition values are important data for setting sintering rates during a ceramic foam sintering process. Agreeing with the results of weight loss, three different sintering processes were operated with 5-5-5, 5-2-5 and 5-0.5-5 ◦C/mim of sintering rates. Ceramic foam structures were monitored via SEM micrographs; the images do not present significant different structures of catalyst sintered with 5-5-5 and 5-2-5◦C/mim. Fig. 8 (b) illustrates the effect of sintering rate on microstructure of ceramic foam catalysts, but the results do not go as expected. From the anticipation, a low sintering rate would aid ceramic foam has enough settling period before a template decomposes, and then the ceramic foam would have high density. In contrast, the structure of catalysts (both PU and PVA) produced from 5-0.5-5 ◦C/mim of a sintering rate is more similar to the original templates [14]. It can be explained that using slow sintering rate causes strut bending, strut melting, the failure of smaller pores, and spot cracking on strut surfaces. Fig. 9 shows that the performance of 10NAM catalysts in DRM reaction. Hydrogen yield of the reaction utilizing 10NAM catalyst sintered with 5-5-5 ◦C/mim of a sintering rate contributes the highest value (around 75%). Relating to the SEM images, it implies that better structure of catalyst foam contributes a higher catalyst activity.

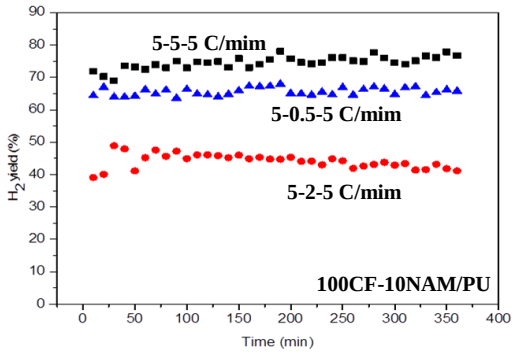

Figure 9. Hydrogen yield from DRM reaction using 100CF-10NAM/PU catalyst

4. Conclusions

An idea to fabricate ceramic foam catalysts for DRM reaction by using an industrial waste polymeric foam template was proposed in this paper, since ceramic foam catalysts provide low pressure drop, high external mass transfer rates, and large efficiency factors for pore-diffusional regimes, etc. All experimental results have led to a greater understanding of a suitable foam structure and catalyst preparation conditions. The results are concluded that PU and VA foam are suitable for the ceramic foam preparation. 10NAM slurry without any dilution provides the highest metal dispersion and catalyst surface area. Sintering rate is significantly important for the performance of ceramic foam catalysts, and 5-5-5 ◦C/mim is the best choice for sintering rate. This paper reported just some part of work, therefore; more information is needed to study for achieving the desired ceramic foam catalysts.

REFERENCES

[1] Rossi,C.C.R.S. Alonso,C.G., Antunes,O.A.C. Guirardello,R. , Cardozo-Filho, L., "Thermodynamic analysis of steam reforming of ethanol and glycerine for hydrogen production," *Inter Journal of Hydrogen Energy*, Vol. 34, pp. 323-332, 2009.

[2] [Afandizadeh, S. and Foumeny, " E.A. Design of packed bed reactors: guides to catalyst shape, size, and loading selection," *Applied Thermal Engineering*, Vol. 21, pp. 669-682, 2001.

[3] Twigg, M.V. and Richardson, J.T., "Theory and applications of ceramic foam catalysts," *Trans IChemE*. Vol. 80, Part A. pp. 183-189, 2002.

[4] Richardson, J.T., Remue, Hung, D. J.-K., "Properties of ceramic foam catalyst supports: mass and heat transfer," *Applied Catalysis A: General*, Vol. 250. pp. 319–329, 2003.

[5] Luyten, J., Mullens,S. Cooymans, De Wilde,J. A.M., Thijs, I., Kemps, R., "Different methods to synthesize ceramic foams," *Journal of the European Ceramic Society*, Vol. 29, pp. 829–832, 2009.

[6] Al-Nakoua, M. A. El-Naas, M. H., Abu-Jdayil, B., "Characterization and testing of sol–gel catalysts prepared as thin layers in a plate reactor," *Fuel Processing Technology*, Vol. 92, pp. 1836–1841, 2001.

[7] Ahmad, H., Saeid, B., Rahmatolah, E., Shirin, N., "Different pore size alumina foams and study of their physical and mechanical properties," *Proceedings of The 2011 IAJC-ASEE International Conference*, 2001, Iran.

[8] Faure, R., Rossignol,F., Chartier, T. Bonhommea,C., Maître, A., Etchegoyen,G. P Gallo,Gary D. D., "Alumina foam catalyst supports for industrial steam reforming processes," *Journal of the European Ceramic Society*, Vol. 31, pp. 303–312, 2001.

[9] Abu-Jdayil, B., Al-Nakoua, M. A., El-Naas, M. H., Khaleel, A., "Rheological characteristics of nickel alumina sol–gel catalyst," *Fuel processing technology*, Vol. 102, pp. 85–89, 2012.

[10] Hayakawa, T, Suzuki, S, Nakamura, J, Uchijima, T, Hamakawa, S, Suzuki, K, Shishido, T., Takehira K., "CO_2 reforming of CH_4 over Ni/perovskite catalysts prepared by solid phase crystallization method," *Applied Catalysis A*, Vol. 183, pp. 273–285, 1999.

[11] Takehira K., "Highly dispersed and stable supported metal catalysts prepared by solid phase crystallization method," *Catalysis Surveys from Japan*, Vol. 6, pp. 19–32, 2002.

[12] Raffaella, V, Cinzia, C, Gianpiero, G, Luca, L, Pio, F, Ugo, C. & Stefano, R., "Ni based mixed oxide materials for CH_4 oxidation under redox cycle conditions," *Journal of Molecular Catalysis A: Chemical*, Vol. 204–205, pp. 637–646, 2003.

[13] Ghislain D.,Esteban, O., Kamel C., Abdelatif M., Bernard , B, "Grafting of phosphonate groups onto PVA by acetalyzation. Evaluation of the anti-corrosive properties for the acetalyzed PVA coatings," *Reactive & Functional Polymers*, Vol. 71, pp. 599–606, 2011.

[14] Wu, K., Park, H-S., Willert-Porada, M., "Pyrolysis of polyurethane by microwave hybrid heating for the processing of NiCr foams," *Journal of Materials Processing Technology*, Vol. 212, pp. 1481– 1487, 2012.